Chemical Engineering Journal 149 (2009) 301–310

Contents lists available at ScienceDirect

Chemical Engineering Journal

journal homepage: www.elsevier.com/locate/cej

Gas void ratio and bubble diameter inside a deep airlift reactor

J.P. Giovannettone[a], E. Tsai[b], J.S. Gulliver[c,*]

[a] Institute of Water Resources, Hydrologic Engineering Center, 609 2nd St. Davis, CA 95616, USA
[b] MWH, 300 N Lake Ave, Pasadena, CA 91101, USA
[c] Department of Civil Engineering, University of Minnesota, Minneapolis, MN 55455, USA

ARTICLE INFO

Article history:
Received 11 December 2007
Received in revised form 27 October 2008
Accepted 9 November 2008

Keywords:
Aeration
Bubble columns
Airlift reactor
Hydrodynamics
Voidage
Bubble size
Gas holdup

ABSTRACT

Void ratio (gas holdup) and bubble diameter measurements were made inside a 1.06-m diameter column containing bubbly flow at depths up to 24 m. Experiments were performed in order to identify differences in trends with column geometry and operating conditions from those found in smaller columns. Void ratio was found to increase as depth decreased regardless of the sparger type or column height. It was also found that larger columns exhibit a wider range of void ratios between the top and bottom than for smaller columns. A straightforward model was developed to predict the void ratio at heights greater than 2 m above the column bottom. The model incorporates the influences of hydrostatic pressure, superficial gas and liquid velocities, and a fitted bulk bubble-rise velocity while ignoring gas transfer with air as the gas of interest. The fitted slip velocities were found to compare well with literature measurements of single-bubble slip velocities. If the void ratio profiles are already known, the equation can also be used to estimate the bubble slip velocity, which is difficult to measure experimentally.

Bubble diameter measurements were made using a submersible camera attached to a trolley. It was found that the Sauter mean bubble diameter does not change with gas flow rate and depth and can decrease substantially when not taking the few largest bubbles (outliers) into account. In contrast, differences were observed when comparing column types. With or without the outliers removed, the bubble column contained larger bubbles than the airlift reactor, which may justify conversion to an airlift reactor and clarify some important factors in the operation of commercial-scale columns.

1. Introduction

Two-phase gas–liquid reactors in industry can be up to 40 m in height with diameters up to 10 m and can be in the form of either a bubble column or an airlift reactor. An airlift reactor is different from a bubble column in that it separates the rising and sinking fluid into two containers, the riser and downcomer, respectively. Both types of reactors are used in several applications, which include the catalytic conversion of hydrocarbons, coal liquefaction, or the synthesis of hydrocarbons from carbon monoxide and hydrogen, absorption processes, extraction, fermentation, among others. There is also interest in boiling gas–liquid flow, such as may occur in a nuclear reactor. Three types of gas–liquid flows may exist in these reactors depending on operating conditions [1]: (1) bubbly flow (up to 0.05–0.08 m/s), where individual bubbles rise with or against the flowing liquid; (2) slug flow, where a bullet shaped Taylor bubble rises at high velocity while shedding smaller bubbles; and (3) annular flow, where a liquid film moves along the wall and a gas core is present inside this film. One important application that operates exclusively in the bubbly flow regime is the use of an airlift reactor to replenish oxygen in the hypolimnion (bottom) of a lake or reservoir [2]. Reoxygenation helps promote the survival of aerobic bacteria, prevent algal blooms and odor problems, and improves living conditions for aquatic life. A typical setup [3] consists of a riser in the middle of the device, which removes the unaerated water from the hypolimnion, and an outer shell where the re-aerated water is returned to the hypolimnion.

The main parameters that characterize the hydrodynamics inside a bubble column are the gas void ratio, mean bubble diameter, mixing, and the volumetric mass transfer rate, while airlift reactors add the liquid circulation velocity. These can be affected by the geometry of the column and the existing operating conditions, of which the gas and liquid flow rates are the most important. Other variables to consider are the properties of the continuous media used inside the reactor and the type of sparger used to introduce gas into the media. The current study will investigate the effects of changing the geometry and operating conditions of a full-scale airlift reactor on the void ratio and mean bubble diameter, with comparisons made to a bubble column. Measurements of void ratio and bubble diameter allow calculations of the interfacial

* Corresponding author at: Department of Civil Engineering, Room 127A, University of Minnesota, Minneapolis, MN 55455, USA. Tel.: +1 612 625 4080; fax: +1 612 626 7750.
E-mail address: gulli003@umn.edu (J.S. Gulliver).

1385-8947/$ – see front matter © 2008 Elsevier B.V. All rights reserved.
doi:10.1016/j.cej.2008.11.024

Nomenclature

a	specific surface area, m^{-1}
A	cross-sectional area, m^2
A_b	bubble surface area, m^2
C	concentration in liquid phase, $kg\,m^{-3}$
C_b	concentration in gas phase, atm
d	bubble diameter, m
D_c	column diameter, m
h	water height, m
H	Henry's Law constant, $atm\,m^3\,kg^{-1}$
K_L	liquid film coefficient, m/s
L	pressure head, m
n	moles of gas in volume V_b
P	pressure, atm
R	universal gas constant, $atm\,m^3\,mol^{-1}\,K^{-1}$
S	estimator of scale
T	absolute temperature, K
u	superficial velocity, m/s
U_s	bubble-rise velocity relative to u_l, m/s
v	velocity of bubbles relative to fixed coordinates, m/s
V_b	bubble volume, m^3
z	vertical coordinate or measurement height
z_s	z-score

Greek symbols

ρ_b	gas density, $kg\,m^{-3}$
φ	gas void ratio
σ	standard deviation of bubble size, m
$\sigma_{\ln}$	standard deviation of the natural log of bubble size

Subscripts

2	2″ pipe
a	mean
atm	local atmospheric
b	Sauter mean
d	downcomer
g	gas
Gas	during gas injection at current pressure tap
Gas-1	during gas injection at pressure tap below current tap
i	index
l	liquid
Post	after gas is shut off at current pressure tap
Post-1	after gas is shut off at pressure tap below current tap
Pre	before gas injection at current pressure tap
Pre-1	before gas injection at pressure tap below current tap
r	riser
s	free surface
Tap	current pressure tap
Tap-1	pressure tap below current tap

surface area of the bubbles, which are important to mass transfer calculations [4].

2. Previous work

A number of studies have been performed in an attempt to design airlift reactors and bubble columns to be more efficient at gas transfer. In order to accomplish this, an estimate of the gas transfer rate needs to be made. A higher gas transfer rate is characterized by a high total interfacial surface area of the bubbles, which requires estimates of void ratio and mean bubble diameter. An important issue is that previous studies have used relatively short columns with the tallest being 10.5 m [5], 7.23 m [6], and 6 m [7]. Results from these studies have shown that column height has a negligible effect on void ratio [8–11]; therefore, an overall void ratio has been calculated for the entire column [12–15]. In contrast, it was found in the present study that gas void ratio does increase with height, which indicates that caution must be taken when extrapolating the results from smaller columns to full-scale column heights.

Results concerning the superficial liquid velocity are more consistent. When varying the liquid circulation velocity from 0 m/s (bubble column) to a positive value (airlift reactor), void ratio has been found to decrease [7,12,15]. Due to the liquid circulation present in an airlift reactor, the down flowing regions near the wall are reduced, which allows bubbles to enter and leave quickly, reducing the void ratio.

A large portion of the volume of the smaller columns is taken up by the sparger zone, which is located above the sparger. The sparger zone is where bubble coalescence and breakup are not in equilibrium and, as a result, where bubble size changes more rapidly with height than throughout the remainder of the column. This will affect the measured bubble size in the smaller columns. Colella et al. [16] measured bubble diameter in two bubble columns of varying heights and diameters and found that bubble size decreased with height in the shorter bubble column, but did not change in the larger bubble column above a height of 0.375 m above the sparger. Polli et al. [17] found similar results and estimated the sparger zone to extend one column diameter above the sparger. In contrast, Ohkawa et al. [18] and Magaud et al. [19] found that bubble diameter changes little with height in columns of comparable size. One explanation for the different observations in the sparger zone is the initial size of the bubbles compared to the dynamic equilibrium of bubble size. If the initial size of the bubbles is smaller than the terminal bubble size, then the trend in bubble size will be increasing in the sparger zone, and vice versa. If the initial bubble size is near the equilibrium size, then a negligible change should be observed with height. The equilibrium size is determined by effects due to shear [20–23], but little work has been done concerning the amount of shear produced in a bubble column.

There are conflicting results in the literature on the effects of changing gas and liquid flow rates upon bubble size. Some studies have found that bubble diameter decreases with superficial gas velocity [24,25], which is due to increased bubble breakup at higher gas flow rates, creating a greater number of smaller bubbles. Miyahara and Hayashino [26] found that mean bubble size decreases with superficial gas velocity at lower velocities (0.003–0.008 m/s) and then increases to an equilibrium diameter at higher gas velocities. In contrast, an increase in superficial gas velocity has also been found to increase bubble diameter [17,19,27,28] or have no effect [7,18,29,30]. In terms of liquid velocity, Colella et al. [16] found that bubble columns ($u_l = 0$) and airlift reactors ($u_l > 0$) produce bubbles of similar sizes throughout the height of the columns.

Further information on the literature comparisons can be found in Giovannettone [31]. It is difficult to make generalizations from these studies due to the multiple variables being altered between experiments [16,17]. The columns used are shorter than most industrial reactors and do not come close to the depths that exist in applications involving lake and reservoir aeration, which leaves unanswered questions about scale-up. The purpose of the current work is to determine the effects of column geometry and specific operating conditions on void ratio and mean bubble diameter in a deep airlift reactor and bubble column (23.4 m) by changing only one parameter between experiments. This will decrease scale-up issues and allow more assertive conclusions to be made than in previous studies. Three column heights and three spargers will be tested. The results are compared to those from previous studies

and used to calculate the interfacial surface area of the bubbles in a parallel study [4].

3. Prediction of void ratio in a tall column

Bubble columns and airlift reactors are known to contain a non-uniform cross-section of bubbles and bubble sizes [32]. Our hypothesis is that, for void ratio, this non-uniform distribution is predominant in the first meter or two of the column, and less important for a column of a height greater than an adult human, i.e., a "tall" column, as long as the sparger is distributed across the bottom of the column. What needs to be considered in a tall column is the effect of pressure and mass transfer [33] on void ratio. Assuming steady-state and a uniform cross-sectional distribution, corresponding to a Zuber and Findlay distribution coefficient of one, a mass balance in one dimension can be written as a sum of gas transfer and pressure effects:

$$\frac{v}{\varphi}\frac{d\varphi}{dz} = \frac{1}{\rho_b \varphi}\sum_{i=1}^{I} K_{Li}a\left(C_i - \frac{C_{bi}}{H_i}\right) - \frac{v}{P}\frac{dP}{dz} \quad (1)$$

where φ is void ratio or gas holdup, v is the velocity of the bubbles relative to fixed coordinates, z is the vertical coordinate, ρ_b is gas density in the bubbles, K_{Li} is the liquid film coefficient for compound i, a is specific surface area (surface area of the bubbles per unit volume), C_i and C_{bi} are the concentration of compound i in the liquid and gas phase, respectively, H_i is Henry's law constant for compound i, R is the universal gas constant, T is absolute temperature and P is pressure. If the impact of gas transfer on void ratio is small, and hydrostatic pressure is assumed ($P = L_{atm} + h - z$), where L_{atm}, h, and z are the atmospheric pressure head, total column height, and measurement height, respectively, Eq. (1) can be reduced to:

$$\frac{d\varphi}{dz} = \frac{\varphi}{L_{atm} + h - z} \quad (2)$$

Integrating Eq. (2) from the free surface to z results in:

$$\varphi = \frac{\varphi_s L_{atm}}{L_{atm} + h - z} \quad (3)$$

where φ_s is the void ratio at the free surface. Following Zuber and Findlay [32] for φ_s with a uniform distribution of bubbles gives,

$$\varphi_s = \frac{u_g}{U_s + u_l + u_g} \quad (4)$$

where U_s is the slip velocity of individual bubbles, and u_l and u_g are the superficial liquid and gas velocities, respectively, at atmospheric pressure. Then, Eq. (3) becomes:

$$\varphi = \frac{L_{atm}}{(L_{atm} + h - z)}\frac{u_g}{(U_s + u_l + u_g)} \quad (5)$$

4. Experimental setup

The experiments take place in a steel standpipe at St. Anthony Falls Laboratory, University of Minnesota (Fig. 1). The standpipe is 26.0 m high with an inner diameter of 1.06 m, and can be filled to a maximum unaerated depth of 23.4 m. The continuous phase used in the column is tap water. The gas used for the experiments is compressed air provided by an air compressor, and the gas flow rate is measured using three rotameters setup in parallel. Due to the large diameter of the column and the limitations of the air compressor, superficial gas velocities remained below 0.013 m/s, which is well within the bubbly flow regime common to the environmental application in lakes and reservoirs.

Three spargers were installed in the column: a perforated plate, a soaker hose, and a coarse-bubble diffuser. The perforated plate consists of a sheet of aluminum positioned 0.46 m above the column floor. The holes in the plate are evenly spaced, with diameters of 4.8 mm and a distance of 7.9 mm between adjacent holes. The perforated plate is designed to cause the injected air to spread uniformly along the cross-sectional area of the column. A soaker hose was also installed to provide small bubbles and is positioned in a ring 0.01 m inside the wall. Soaker hoses are commonly made from recycled tires or plastics and used to distribute water slowly to terrestrial plants. They have recently found application in lakes and reservoirs as an effective means of distributing small bubbles over a large plane area [34]. The final sparger used, the coarse-bubble diffuser, was positioned at the center of the column on the perforated plate. The bubbles from this sparger initially are much larger in size than the bubbles created by the soaker hose and the perforated plate but quickly breakup due to shear. The application of a coarse-bubble diffuser enables a high gas flow rate with minimal pressure loss.

Experiments were performed with or without a throughput of liquid to simulate an airlift reactor and a bubble column, respectively. Three 0.31 m baffles, designed to allow only water flow, are located at heights of 6.0, 10.0, and 23.0 m above the column floor and attached to three downcomer pipes, which are opened and closed using butterfly valves to create varying total column heights. The water exits through one of the baffles and reenters the reactor near the column floor. Liquid circulation is controlled by a pump and gate valve near the bottom of the column. More details about the experimental setup can be found in Giovannettone [31].

5. Measurements

The various combinations of operating conditions tested resulted in 110 void ratio and 36 bubble diameter experiments. Initial measurements of atmospheric pressure, water column height, liquid velocity, column water temperature, and the air temperature outside the column were made prior to each void ratio experiment.

5.1. Void ratio measurements

Measurements of pressure drop were made using six pressure taps located at heights of 0, 2, 5, 9, 16 and 22 m above the column floor (Fig. 1). The taps are connected by 0.635-cm plastic tubing to a

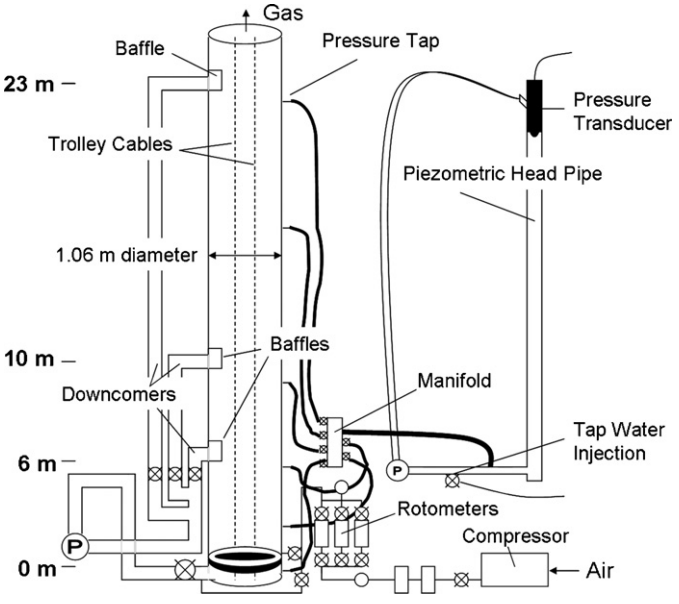

Fig. 1. Schematic of reactor setup for void ratio experiments.

0.051-m PVC pipe (referred to as the pressure pipe) that extends up the side of the column. A Druck pressure transducer positioned near the top of the pipe provides pressure measurements that, when divided by the specific gravity of the water, will be used to compute the level of the non-aerated water surface. Specific gravity is determined by measuring water temperature inside the pipe using a thermocouple connected to a data logger. In order to prevent temperature variations inside this thin pipe, water is circulated using a small pump and hose.

The pressure transducer was initially submerged in the pressure pipe and calibrated to the water surface elevation without bubbles present. The main column was filled with water until the water surface was 3–4 cm above the transducer measuring point. The pump was then turned on for at least 20 min to create a uniform temperature profile throughout the bubble column and the recirculation pipes. Three pressure measurements were taken at each pressure tap: pre-gas, gas, and post-gas. The results from each individual run were analyzed to determine a steady-state water surface level using a first-order relationship that represents a solution of the energy equation between the pressure pipe and the main column while taking into account head loss in the pressure tap tubing and assuming the flow in the tubing is laminar [31]. The void ratio (φ) was calculated assuming hydrostatic pressure, giving equal weight to the pre-gas and post-gas measurements:

$$\varphi = 100\left[1 + \left(\frac{\rho_2}{\rho_r}\left(\frac{[(L_{Gas} - L_{Pre}) - (L_{Gas\text{-}1} - L_{Pre\text{-}1})] + [(L_{Gas} - L_{Post}) - (L_{Gas\text{-}1} - L_{Post\text{-}1})]}{2(h_{Tap} - h_{Tap\text{-}1})} - 1\right)\right)\right] \quad (6)$$

where ρ_2 and ρ_r are the densities of the water in the 2″ pipe and the bubble column, respectively; L_{Gas}, L_{Pre}, and L_{Post} are the pressure head measurements at a specific tap during gas, pre-gas, and post-gas conditions, respectively; $L_{Gas\text{-}1}$, $L_{Pre\text{-}1}$, and $L_{Post\text{-}1}$ are the pressure head measurements taken from the tap below the current tap during gas, pre-gas, and post-gas conditions, respectively; and h_{Tap} and $h_{Tap\text{-}1}$ are the heights of the current tap from which measurements are being taken and one tap below, respectively.

5.2. Bubble diameter measurements

The specific setup for measuring bubble diameter consists of a submersible video camera positioned on a trolley apparatus (Fig. 2) that can be moved vertically in the column on a nylon rope and two galvanized steel cables and contains a 5 cm opening through which the bubbles will rise. A strobe light allows still images to be taken from the camera, which is located 15 cm from bubbles and is connected to a processor to save the images on a tape in digital format.

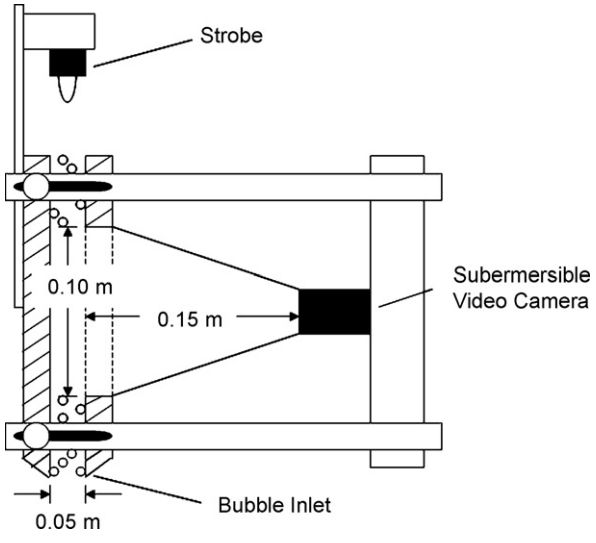

Fig. 2. Schematic of chamber for bubble diameter measurements.

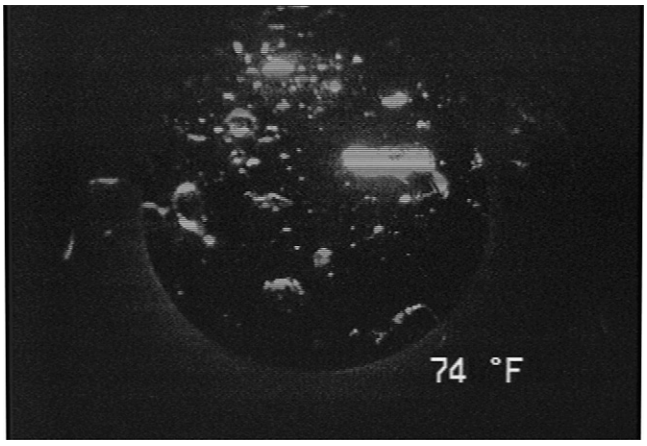

Fig. 3. Example of a picture taken inside the column (u_g = 0.0088 m/s, height = 21.0 m, diffuser = coarse-bubble, column type = airlift reactor, total column height = 23.4 m).

During data collection, the camera was allowed to record for approximately 2 min. The videos were downloaded to a computer, and individual frames were randomly chosen for analysis. An example of one such image is shown in Fig. 3. Each image was then corrected for distortion using *Adobe Photoshop*. The amount of distortion was determined by videotaping a grid of squares with known dimensions, from which a set of correction coefficients was determined and used on succeeding images. The grid was also used to create a pixel to cm conversion factor for each length measurement. The major and minor axes of each bubble in the corrected images were measured by fitting ellipses over them using the image analysis software, *ImageJ*. Assuming each bubble is symmetrical about the minor axis, bubble volume can then be calculated. The radius of a sphere of equal volume was then calculated.

Between 100 to over 200 individual bubble measurements were taken depending on the range of bubble sizes observed during each experiment and at each location. This number of measurements is common for statistical purposes [13,25,26,35,36], while others have used at least 500 [16] and 600 [17] bubbles per sample, especially near the sparger. After the bubbles were measured, the Sauter mean diameter was calculated for each set of conditions in order to weight the results by the bubble interfacial surface area using the following equation [24]:

$$d_b = \frac{6\sum V_b}{\sum A_b} \quad (7)$$

where V_b and A_b are the volume and surface area of each bubble, respectively.

Two possible sources of error that could affect the final results are the shading or blocking of small bubbles by larger bubbles and the distortion of the bubble sizes by wall effects inside the bubble measuring chamber and by the camera. Regarding blocking, it has been assumed that because the flow is in the bubbly flow regime, the bubbles are about the same size. Ignoring the shading of smaller bubbles in the 5 cm wide bubble channel will cause a slight bias toward the larger bubbles, but this effect will be lessened when computing Sauter mean diameter, which is already weighted

towards the larger bubbles. In order to account for the distortion of the bubble size by the wall effects of the measuring chamber and by the camera, a preliminary test was performed inside a small chamber using the submersible camera under dark conditions and the digital video camera under light conditions. A small bubble plume was created using a porous stone. After estimating the Sauter mean diameter of 50 bubbles during each test, it was found that measurements using the submersible camera were 1.9% less than when the digital camera was used. Therefore, wall effects and image analysis using the submersible camera have a small effect on bubble diameter measurements.

5.3. Bubble diameter outlier detection

An outlier technique was used to remove large bubbles when making comparisons within one experiment, where the appearance of one large bubble can distort the comparisons. This technique involves using the median of the data and the absolute deviation of each data point from the median to determine if it is an outlier [37,38]. After the median and deviations are calculated, the median of the absolute deviations is found. An estimator of scale (S) is then calculated by multiplying the median of the deviations by 1.483 to make it consistent with the standard deviation from a normal distribution. A z-score is finally determined using the following equation:

$$z_s = \frac{d_i - median(d_i)}{S}, \quad (8)$$

where d_i is the measured diameter of each bubble. A z-score threshold is then set so that any bubble diameter measurement having a z-score above this threshold is not included in the Sauter mean diameter calculation. As in Urban et al. [37], a threshold of $z_s = 2.5$ was used, which corresponds to a confidence interval of 98.7% for a Gaussian distribution. The Sauter mean diameter was then recalculated. This technique was used when focusing on the variation of bubble diameter with column height, but when comparing sparger types, column types, and the total unaerated water depth and comparing the results with those in the literature, the outliers were included in the analysis.

6. Results/discussion

6.1. Void ratio

Before any void ratio experiments were performed, a measurement uncertainty analysis was incorporated [39]. Fig. 4 shows the results of the uncertainty analysis on five experimental runs performed at a superficial gas velocity of 0.67 cm/s. Void ratio increases with height to a value at the top of the column over 1.6 times what it was near the bottom of the column. Measurement uncertainty analyses were not performed under other operating conditions, but the results from this analysis should give a general estimate of uncertainty for succeeding experiments.

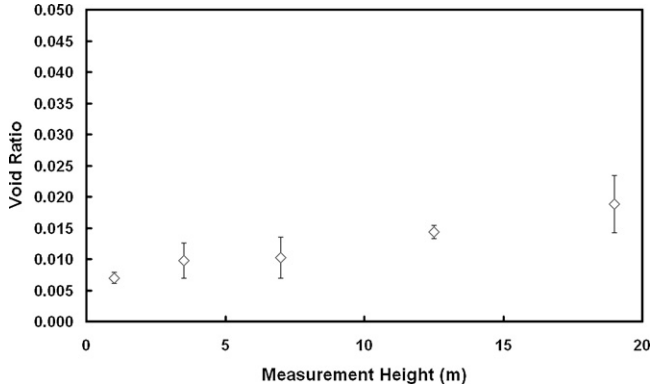

Fig. 4. Void ratio found using the steady-state method with uncertainty to the 95% confidence level under the following operating conditions: column height = 23.4 m, sparger = perforated plate, column = airlift reactor, u_g = 0.67 cm/s.

Table 1
Bubble-rise velocities from a best-fit of Eq. (5) to Fig. 7 data.

Operating conditions	U_s (m/s)
EALR, plate, 23.4 m	0.25
EALR, soaker, 23.4 m	0.24
EALR, coarse, 23.4 m	0.23
BC, plate, 23.4 m	0.22
EALR, plate, 10.6 m	0.185

Results for all void ratio experiments excluding the 6.6 m column are given in Fig. 5a–e. These figures show that void ratio increases with height regardless of the sparger type and column height, unlike what is reported in much of the literature for smaller columns. Agreement with the literature is seen in Fig. 5a and 5d where the void ratio is observed to be lower in the airlift reactor than in the bubble column.

Bubble slip velocity, U_s, in Eq. (5) was fitted to the data above the first measurement height where void ratio had reached an apparent stability. The results are shown in Table 1. It can be observed that the fit gives a gas slip velocity of 0.24 ± 0.01 m/s for all sparger types in the 23.4-m airlift reactor. A lower slip velocity was estimated in the bubble column (0.22 m/s), which is consistent with the findings of Shimizu et al. [15]. The simple model of Eq. (5) fits the data well except at the lowest depths where the void ratios are overestimated. A possible explanation is that bubble-rise velocities near the bottom are greater due to an uneven distribution of the bubbles over the cross-section, creating columns of bubble-water jets/plumes. Another possibility is the non-uniform bubble size distribution, although this would be greatest for the coarse-bubble diffuser, and there is no indication that the data in Fig. 5c is different from the other airlift reactor experiments. A third possibility is that the gas transfer rates up to a column height of 3.5 m may be greater in the airlift reactor due to the advection of less concentrated water from the top of the column. The gas transfer effect, however, would bring the void ratio consistently down throughout the height of the column. The measured void ratio would only match the model at the top of the column where sufficient degassing of the water back into the bubbles has caused the DO concentration to equal that of the water being advected down to the bottom of the column. Therefore, the uneven distribution of bubbles near the bottom of the column is the likely cause, because the model fits the measurements well at all other heights.

The fitted U_s values were also compared to the single-bubble slip velocities in tap water measured by Haberman and Morton [40] (Fig. 6). The comparison indicates that the model of Eq. (5), applied to the void ratio measurements of this study, can be used to estimate bubble slip/rise velocity with relative accuracy. The lowest bubble slip velocity of 0.185 m/s, found for the 10.6-m airlift reactor, is below the results of Haberman and Morton [40], which is likely caused by the low resolution of the fit (2 data points). The reasonable fit suggests that superficial gas and liquid velocities, bubble slip velocity, and a pressure correction term are sufficient to predict gas void ratio in industrial-scale reactors without significant reaction rates.

The results from previous studies in the literature are divided between those performed in a bubble column and those performed in an airlift reactor and are shown in Fig. 7, with the range of geometry and operating conditions of the columns used given in Table 2. Also shown in Fig. 7 are the results of the current study for the

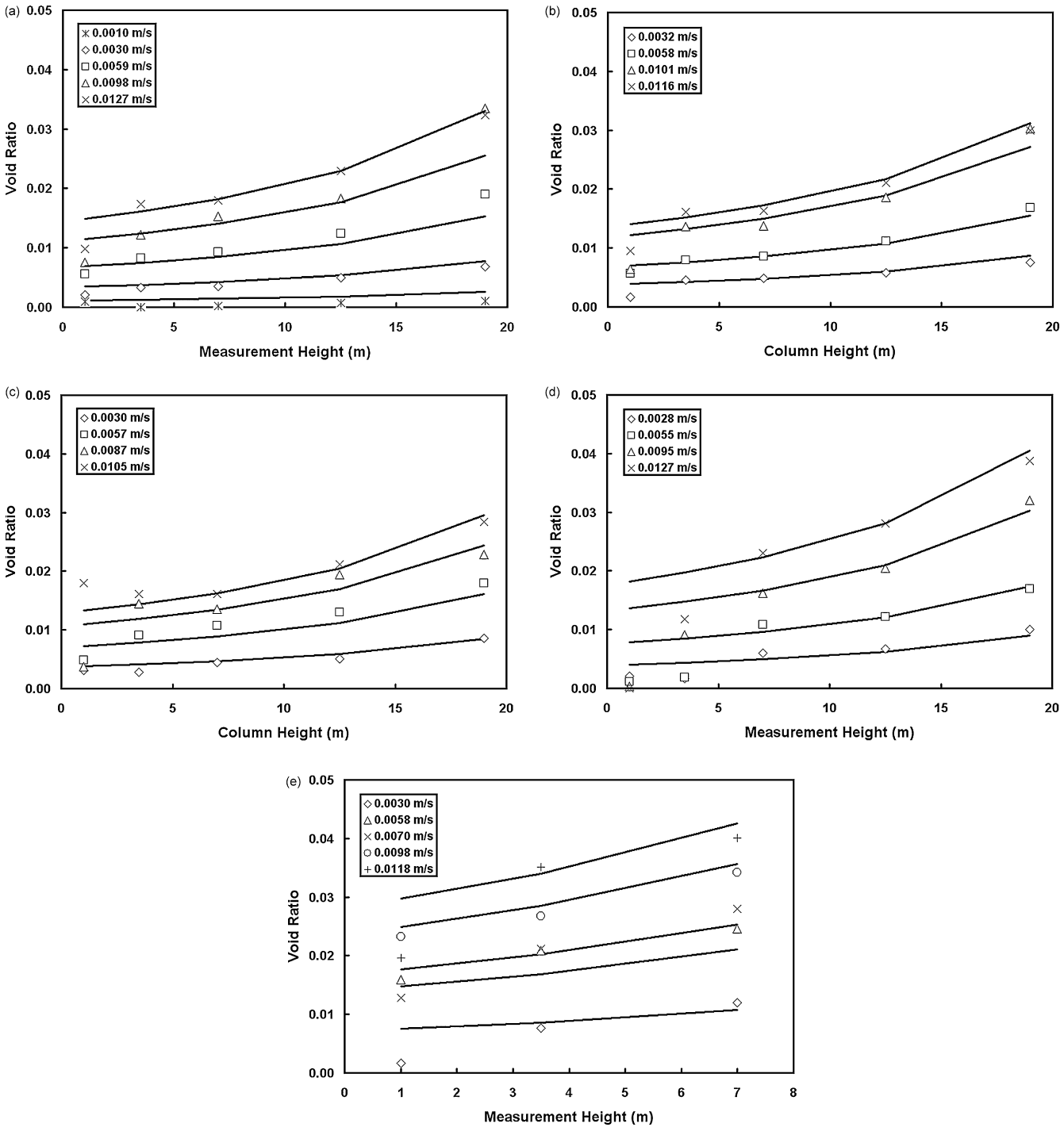

Fig. 5. Void ratio vs. height at various superficial gas velocities under the following operating conditions: (a) airlift reactor, 23.4 m, plate, (b) airlift reactor, 23.4 m, soaker hose, (c) airlift reactor, 23.4 m, coarse-bubble diffuser, (d) bubble column, 23.4 m, plate, and (e) airlift reactor, 10.6 m, plate. Lines represent fit of Eq. (5) to upper measurement heights.

10.6 and 6.6 m columns. Two key observations may be made from Fig. 7: (1) the slope of void ratio with u_g is greater for the studies that used a bubble column than for those that used an airlift reactor, which is consistent with the results of the present study, and (2) the void ratio results measured closer to the top of the 10.6 m EALR in the present study give results above the literature values, while those closer to the bottom consistently give void ratios below that of the literature. This demonstrates that the variation in void ratio between the top and bottom of the reactor increases as larger columns are used. Such a result suggests that using the results of shorter columns to assign a single void ratio to an industrial-scale column may introduce substantial errors away from the middle of the column.

Fig. 8 uses Eq. (5) in an attempt to predict the results of a few of the studies included in Fig. 7. The bubble slip velocity was adjusted for each study in order to obtain an optimal fit. As shown in Fig. 8, Eq. (5) fits the data well. The fitted values of the bubble slip velocity for each study are shown in the legend of Fig. 8 and tend to range from 0.160 to 0.190 m/s, which is around the value estimated for the 10.6 m EALR in the present study (0.185 m/s). The slip velocity estimated for Vial et al. [6] was substantially lower (0.09 m/s), which is a result of the high liquid circulation velocities that were present

Table 2
Operating conditions for void ratio measurements from this and other studies. Measurement height is equal to h_r unless otherwise stated. (h_r = column height, D_c = column diameter, A_d/A_r = ratio of downcomer and riser cross-sectional areas, BC = bubble column, EALR = external airlift reactor, IALR = internal airlift reactor).

Ref.	Col. type	h_r (m)	$D_c \times 10^2$ (m)	u_l (m/s)	Sparger	Pore size $\times 10^3$ (m)	# of Pores	A_d/A_r
[35]	BC	2.00	10.0	0	Nozzle	5.0	1	–
[35]	BC	2.00	10.0	0	Mult. orifice	1.0	62	–
[35]	BC	2.00	10.0	0	Porous plate	.010–.016	Many	–
[6]a	BC	7.23	20.0	0	Mult. nozzle	1.0	56	–
[6]b	BC	4.40	15.0	0	Porous plate	0.15	Many	–
[13]	BC	4.50	20.0	0.64–2.16	Perf. plate	2.5	>1000	–
[14]	BC	3.00	5.0	0	Orifice plate	2.0	1	–
[14]	BC	3.00	23.0	0	Perf. plate	2.0	19	–
[15]	BC	0.83	15.5	0	Perf. plate	1.0	57	–
[15]	EALR	0.80	15.5	–	Perf. plate	1.0	57	0.204
[7]	EALR	6.00	15.0	10.0–17.5	Mult. orifice	1.0	60	0.530
[25]	IALR	1.20	13.7	–	Perf. ring	1.0	14–30	0.07–1.00
Current	EALR	10.60	106.0	0.02	Perf. plate	4.8	>200	0.072

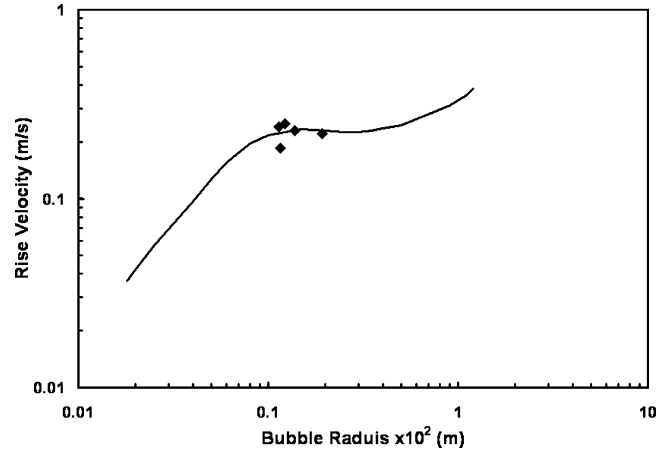

Fig. 6. Terminal bubble-rise velocity as a function of bubble radius. Dots represent data taken from the current study, and the solid line represents best-fit of single bubble-rise velocities measurements from Haberman and Morton [40].

in these experiments. Fits for columns less than 4 m tall (not shown) were not as good, which is assumed to be a result of the effect of the proximity of the sparger to the void ratio measurement locations.

6.2. Sauter mean bubble diameter

6.2.1. Variation with location

Fig. 9 provides a comparison of the Sauter mean bubble diameter in the EALR with height and superficial gas velocity for the coarse-bubble diffuser when outliers are included (Fig. 9a) and omitted (Fig. 9b). The impact a few large bubbles have on the scatter of the bubble diameter results can be seen. At u_g = 0.0088 m/s and a height of 10 m, the Sauter mean diameter for the coarse-bubble diffuser is 3.66 mm (Fig. 9a), whereas when outliers are removed, the Sauter mean diameter drops 27% to 2.68 mm (Fig. 9b). A more detailed comparison for all values of u_g and column height is shown in Table 3 and demonstrates that this distortion can occur at all depths. Once the small numbers of outlier bubbles are removed, Fig. 9b shows that there is no trend of the Sauter mean bubble diameter with measurement height and u_g (up to 0.01 m/s) for all sparger and column types. Therefore, the Sauter mean diameters for each set of experiments (sparger type, column type, and total column height) at all measurement heights and gas flows were averaged for the remaining comparisons.

6.2.2. Type of sparger

An almost equal number of bubble diameter measurements (between 679 and 1823), including outliers, were then taken from each set of experiments. Table 4 displays the number of bubbles measured and the Sauter mean bubble diameter and standard deviation for each sparger. Log-normal bubble size distributions, as presented in Giovannettone [31], were assumed [17,18,26,29,41]. The standard deviation was computed from the standard deviation of the log-normal distribution using the following equation [42]:

$$\sigma = d_a \left[\exp(\sigma_{\ln}^2) - 1\right] \quad (9)$$

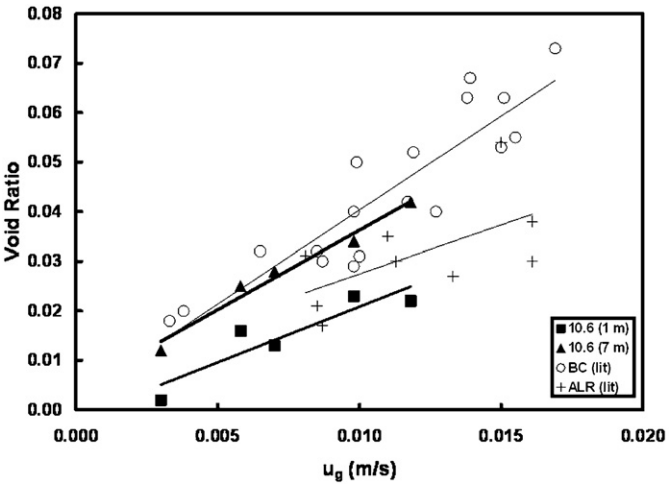

Fig. 7. Literature results from Table 2 (light symbols) compared with results from the current study (dark symbols) for the 10.6 m column EALR.

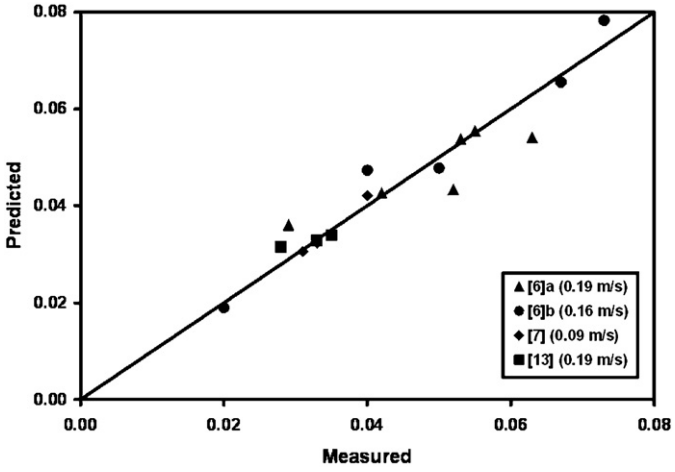

Fig. 8. Fitted vs. measured void ratio values for three studies listed in Table 2. The velocities shown in the legend are the bubble slip velocities required to produce the best-fit for each study.

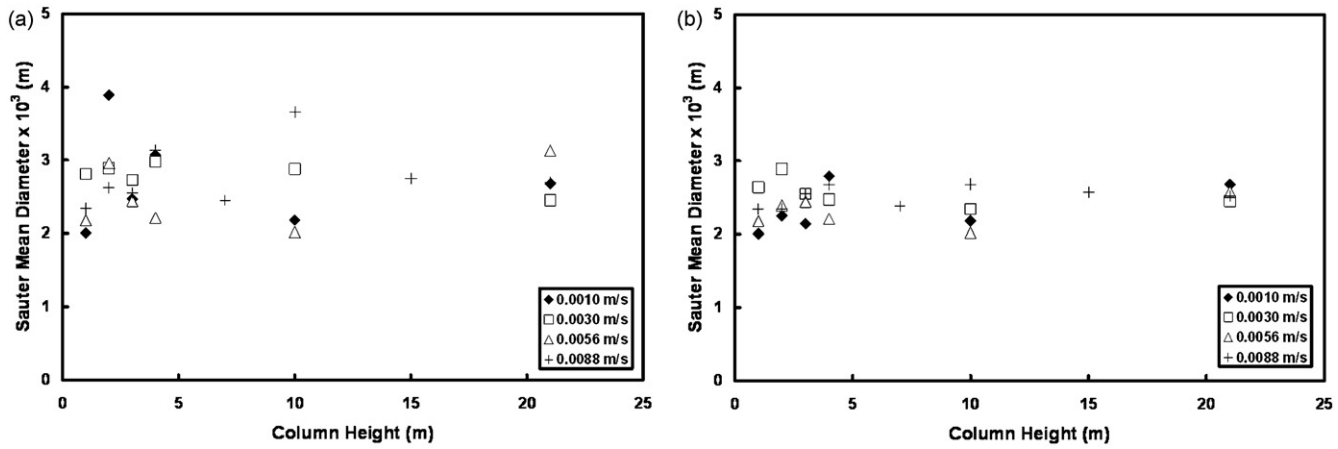

Fig. 9. Bubble diameter measurements (a) before and (b) after the removal of outliers for the following operating conditions: airlift reactor, coarse-bubble diffuser, 23.4 m total depth.

Table 3
Statistics for Sauter mean bubble diameter (d_b) before and after outlier removal for the operating conditions mentioned in Fig. 4.

u_g (m/s)	Distance from sparger (m)	$d_b \times 0^3$ before/after (m)	Stan. Dev. $\times 10^3$ before/after (m)	Bubbles measured (outliers detected)
0.0010	1	2.01/2.01	0.89/0.89	158 (0)
"	2	3.89/2.25	2.08/1.06	97 (2)
"	3	2.47/2.14	1.15/0.96	349 (2)
"	4	3.07/2.79	1.52/1.34	220 (1)
"	10	2.18/2.18	0.97/0.97	129 (0)
"	21	2.68/2.68	1.26/1.26	118 (0)
0.0030	1	2.81/2.64	1.29/1.19	236 (1)
"	2	2.89/2.89	1.42/1.42	243 (0)
"	3	2.73/2.55	1.27/1.16	223 (1)
"	4	2.98/2.47	1.42/1.14	241 (1)
"	10	2.88/2.34	1.29/0.98	215 (3)
"	21	2.45/2.45	1.14/1.14	209 (0)
0.0056	1	2.18/2.18	0.92/0.92	300 (0)
"	2	2.96/2.39	1.40/1.04	239 (5)
"	3	2.44/2.44	1.11/1.11	97 (0)
"	4	2.21/2.21	0.91/0.91	184 (0)
"	10	2.02/2.02	0.83/0.83	133 (0)
"	21	3.13/2.58	1.46/1.17	421 (2)
0.0088	1	2.34/2.34	1.01/1.01	225 (0)
"	2	2.62/2.34	1.13/0.96	216 (3)
"	3	2.55/2.55	1.21/1.21	210 (0)
"	4	3.14/2.68	1.50/1.22	255 (2)
"	7	2.45/2.38	1.05/1.01	220 (1)
"	10	3.66/2.68	1.86/1.32	241 (1)
"	15	2.75/2.57	1.28/1.18	279 (1)
"	21	2.70/2.52	1.23/1.12	234 (1)

where d_a is the mean bubble diameter and $\sigma_{\ln}$ is the standard deviation of the natural logs of the bubble diameters. Table 4 indicates that the type of sparger does have an influence on the mean bubble size and the range of bubble sizes when larger bubbles are considered, which supports the conclusion that increasing pore size and decreasing the number of pores (such as with the coarse-bubble diffuser) causes bubbles to be up to 0.5 mm larger [13,17]. Table 4 also indicates that the difference, or bias, in bubble size between sparg-

Table 4
Sauter mean bubble diameters and standard deviations calculated from the standard deviations of the log-normal distributions for all sets of operating conditions.

Operating conditions	Number of bubbles (outliers)	$d_b \times 10^3$ (m) with outliers retained	$d_b \times 10^3$ (m) with outliers removed	Stan. Dev. $\times 10^3$ (m)
Sparger type				
Perf. plate	1812 (9)	2.44	2.30	0.95
Soaker hose	1823 (0)	2.28	2.28	1.01
Coarse bubble	1822 (9)	2.76	2.37	1.30
Column type				
EALR	1387 (7)	2.50	2.36	0.92
BC	1392 (6)	3.84	2.79	1.94
Depth (Perf. plate)				
23.4 m	679 (2)	2.53	2.41	1.01
10.6 m	685 (0)	2.32	2.32	1.02
6.6 m	683 (25)	2.60	2.41	0.71

Table 5
Operating conditions during bubble diameter measurements from other studies. (h_r = column height, D_c = column diameter, A_d/A_r = ratio of downcomer to riser cross-sectional area).

Label	Ref.	Col. type	h_r (m)	$D_c \times 10^2$ (m)	Sparger	Pore size $\times 10^3$ (m)	# of Pores	A_d/A_r	Meas. Ht. (m)
(a)	[18]	BC	2.0	5,6,7	Nozzle	13–25	1	–	1.0
(b)	[25]	IALR	1.2	13.7	Perf. ring	1	14	1	0.1
(c)	[25]	IALR	1.2	13.7	Perf. plate	1	14	1	0.5
(d)	[25]	IALR	1.2	13.7	Perf. plate	1	14	1	0.9
(e)	[25]	IALR	1.2	13.7	Perf. plate	1	14	0.43	0.1
(f)	[13]	BC	4.5	20	Perf. plate	2.5	>1000	–	2.0
(g)	[29]	BC	2.16	56	Nozzles	4	13	–	0.8,1.1,1.4
(h)	[14]	BC	3	5	Orifice plate	2	–	–	All
(i)	[14]	BC	3	23	Perf. plate	2	19	–	All
G1	Current	EALR	23.4	106	Soaker hose	<1	>1000	0.072	1,2,4,10,21
G2	Current	EALR	23.4	106	Perf. plate	4.8	>200	0.072	1,2,4,10,21
G3	Current	EALR	23.4	106	Coarse	–	–	0.072	1,2,4,10,21
G4	Current	BC	23.4	106	Perf. plate	4.8	>200	0.072	7,10,15,21
G5	Current	EALR	10.6	106	Perf. plate	4.8	>200	0.072	Bottom, top
G6	Current	EALR	6.6	106	Perf. plate	4.8	>200	0.072	Bottom, top

ers is due to the few largest bubbles that were earlier excluded as outliers.

6.2.3. Total column height

Table 4 shows that with or without outlier removal, the Sauter mean bubble diameter does not vary substantially between the three column sizes. There is some difference near the sparger, but relative to comparisons with other studies, where Sauter mean diameters of up to 10 mm were measured, these differences of 0.28 and 0.09 mm for detection with and without outliers included, respectively, are small. The standard deviations of bubble sizes in Table 4 demonstrate a decrease from 1.0 for 10.6 and 23.4 m tall columns to 0.7 for 6.6 m tall columns. These results show that the Sauter mean bubble diameter does not depend on the total unaerated height of the column while the distribution of bubble sizes does exhibit some dependence.

6.2.4. Bubble column versus airlift reactor

Table 4 shows that the standard deviation in the bubble column is over twice that in the airlift reactor. Table 4 also reveals that the bubble column produces bubbles that are 54% larger than those measured in the airlift reactor when outliers are included. When the largest bubbles are removed, the bubbles produced in the bubble column remain larger. This is in contrast to the findings of Colella et al. [16] who found no difference in average bubble diameter between the two column types. One possible explanation for the larger mean and range of bubble sizes in the bubble column is that as the bubbles rise they move into the middle of the column where the cross-sectional area of the rising fluid decreases and the velocity increases. The rising fluid may then approach chug-turbulent flow where many larger bubbles are formed. The airlift reactor has minimal negative velocities and is presumed to be better at distributing bubbles across the flow. This hypothesis is reinforced by the fact that the Sauter mean bubble diameter for the bubble column drops from 3.84 to 2.79 mm after outlier removal.

6.2.5. Comparison with other studies

Fig. 10 compares the results (outliers included) with those from other studies, and Table 5 describes the geometry of the columns and the operating conditions for each study. It can be seen that the results and trends from Ohkawa et al. [18] and Luewisutthichat et al. [29] are similar to ours for the bubble column, while Patel et al. [14] obtained similar results to the airlift reactor. Moustiri et al. [13] also obtained similar values of the Sauter mean diameter, but observed a small increasing trend with u_g. Another important point can be made using points (b), (c), and (d) in Fig. 12 from Wongsuchoto et al. [25]. The Sauter mean diameter appears to increase almost 4 mm as the bubble rises from a height of 0.1–0.5 m, and then decreases about 4 mm as the bubble rises to 0.9 m. No such trend was found in the current study. Overall, it was also found that, excluding the low values by Patel et al. [14], the Sauter mean bubble diameter is almost constant in the literature as the total column height is varied with an average size around 4.00 mm. This value matches the mean diameter calculated in the present study for the bubble column when outliers are included, while the Sauter mean diameters in the airlift reactors are lower.

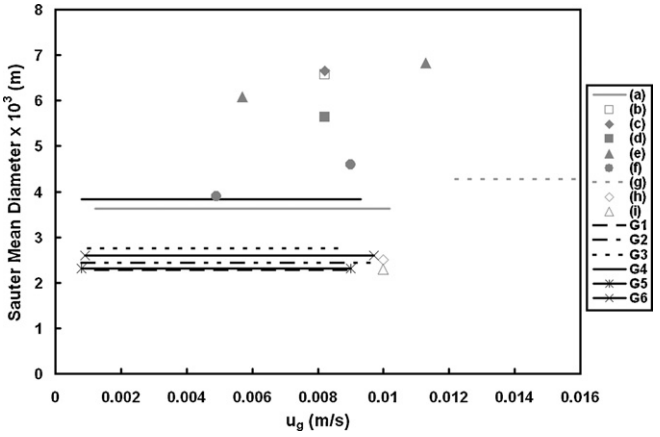

Fig. 10. Sauter mean diameter vs. superficial gas velocity from this study (black symbols) and from the literature (gray symbols). Symbols are identified in Table 5.

7. Conclusions

Void ratio and bubble diameter experiments were performed in a deep reactor to determine the robustness of results obtained from similar experiments performed on bubbly flow in smaller columns. The experiments involved variations in column geometry and operating conditions, including such variables as total column height, superficial gas and liquid velocity, and sparger pore size and density.

The final results indicated some discrepancies with previous studies that have performed similar experiments in smaller columns. It was found that the void ratio increases with column height regardless of sparger type or column size, with taller columns experiencing a larger difference in void ratio between the top and bottom than in smaller columns. An assumed constant void ratio throughout the column, as has been done in the past, will cause larger errors as column size is increased to industrial-scales. An equation was developed and used to accurately predict the bubble slip velocity under various operating conditions. Using this equa-

tion, the bubble slip velocity, superficial gas and liquid velocities, and a pressure correction term are sufficient to predict the void ratio profile along the height of the column, as long as reaction rates are relatively small. Also, if the void ratio profiles are known, the equation can be used to estimate the bubble slip velocity, as was successfully done in the present study. The bubble slip velocity is a difficult quantity to otherwise measure accurately.

With respect to bubble diameter, it was found that after eliminating a few outlier bubbles, bubble diameter does not vary with depth or gas flow rate under all operating conditions except near the sparger. A trend that has been found to occur in the sparger zone, as in some studies [25], does not demonstrate that the same trend will exist throughout the rest of the column. Removing a few large outliers caused the Sauter mean diameter to decrease by up to 27%. Caution should be taken when identifying trends in bubble diameter, because these trends may be due to a few large bubbles. On the other hand, a trend was found when comparing the airlift reactor to the bubble column. Bubbles measured in the bubble column were substantially larger with or without outliers included, which is in contrast to the literature [16]. This result may provide justification for expenditures required to convert a bubble column into an airlift reactor.

The results of this study provide additional insights into basic trends in void ratio and bubble diameter that can be observed in a full-scale airlift reactor and bubble column. Because few experiments have been performed in full-scale reactors, the data and associated analysis obtained in this study is needed and important for the development of design characterizations of deep airlift reactors and bubble columns that can be applied to most field-scale and industrial-scale reactors with few scale-up issues.

Acknowledgements

The authors wish to thank the Chicago District and the Engineering Research and Development Center of the U.S. Army Corps of Engineers for the necessary funding for this research in the form of a research grant, Grant W81EWF-4166-7569, and for the financial support of the “Graduate Assistance in Areas of National Need” under the U.S. Dept. of Education in the form of a research fellowship. The authors would also like to thank Ben Erickson, F. K. Lim, and the shop crew at St. Anthony Falls Laboratory for the setup that made this study possible.

References

[1] Y.T. Shah, B.G. Kelkar, S.P. Godbole, W.D. Deckwer, Design parameters estimations for bubble column reactors, AIChE J. 28 (1982) 353–379.
[2] V.L. Singleton, J.C. Little, Designing hypolimnetic aeration and oxygenation systems—a review, Environ. Sci. Technol. 40 (2006) 7512–7520.
[3] J.C. Little, Hypolimnetic aerators—predicting oxygen transfer and hydrodynamics, Water Res. 29 (1995) 2475–2482.
[4] J.P. Giovannettone, J.S. Gulliver, Gas transfer and liquid dispersion inside a deep airlift reactor, AIChE J. 54 (2008) 850–861.
[5] J.H. Hills, The operation of a bubble column at high throughputs. I. Gas hold-up measurements, Chem. Eng. J. 12 (1976) 89–99.
[6] W.-D. Deckwer, R. Burckhart, G. Zoll, Mixing and mass transfer in tall bubble columns, Chem. Eng. Sci. 29 (1974) 2177–2188.
[7] C. Vial, S. Poncin, G. Wild, N. Midoux, Experimental and theoretical analysis of the hydrodynamics in the riser of an external loop airlift reactor, Chem. Eng. Sci. 57 (2002) 4745–4762.
[8] J.R. Fair, A.J. Lambright, J.W. Andersen, Heat transfer and gas holdup in a sparged contactor, Ind. Eng. Chem. Process Des. Dev. 1 (1962) 33–36.
[9] H. Hikita, S. Asai, K. Tanigawa, K. Segawa, M. Kitao, Gas hold-up in bubble columns, Chem. Eng. J. 20 (1980) 59–67.
[10] D. Pfleger, S. Becker, Modelling and simulation of the dynamic flow behaviour in a bubble column, Chem. Eng. Sci. 56 (2001) 1737–1747.
[11] U.P. Veera, J.B. Joshi, Measurement of gas hold-up profiles by gamma ray tomography: effect of sparger design and height of dispersion in bubble columns, Chem. Eng. Res. Des. 77 (1999) 303–317.
[12] K. Akita, T. Okazaki, H. Koyama, Gas holdups and friction factors of gas–liquid two-phase flow in an air-lift bubble column, J. Chem. Eng. Jpn. 21 (1988) 476–482.
[13] S. Moustiri, G. Hebrard, M. Roustan, Effect of a new high porosity packing on hydrodynamics of bubble columns, Chem. Eng. Process. 41 (2002) 419–426.
[14] S.A. Patel, J.G. Daly, D.B. Bukur, Holdup and interfacial area measurements using dynamic gas disengagement, AIChE J. 35 (1989) 931–942.
[15] K. Shimizu, S. Takada, T. Takahashi, Y. Kawase, Phenomenological simulation model for gas hold-ups and volumetric mass transfer coefficients in external-loop airlift reactors, Chem. Eng. J. 84 (2001) 599–603.
[16] D. Colella, D. Vinci, R. Bagatin, M. Masi, E.A. Bakr, A study on coalescence and breakage mechanisms in three different bubble columns, Chem. Eng. Sci. 54 (1999) 4767–4777.
[17] M. Polli, M. Di Stanislao, R. Bagatin, E. Abu Bakr, M. Masi, Bubble size distribution in the sparger region of bubble columns, Chem. Eng. Sci. 57 (2002) 197–205.
[18] A. Ohkawa, Y. Kawai, D. Kusabiraki, N. Sakai, D. Endoh, Bubble size, interfacial area and volumetric liquid-phase mass transfer coefficient in downflow bubble columns with gas entrainment by a liquid jet, J. Chem. Eng. Jpn. 20 (1987) 99–101.
[19] F. Magaud, M. Souhar, G. Wild, N. Boisson, Experimental study of bubble column hydrodynamics, Chem. Eng. Sci. 56 (2001) 4597–4607.
[20] J.O. Hinze, Fundamentals of the hydrodynamic mechanism of splitting in dispersion processes, AIChE J. 1 (1955) 289–295.
[21] M. Sevik, S.H. Park, The splitting of drops and bubbles by turbulent fluid flow, J. Fluids Eng. 95 (1973) 53–60.
[22] J.M. Killen, An experimental investigation of the influence of an air bubble layer on radiated noise and surface pressure fluctuations in a turbulent boundary layer, in: Report #202, Saint Anthony Falls Laboratory, University of Minnesota, Minneapolis, MN, 1981.
[23] P.M. Wilkinson, A.V. Schayk, J.P.M. Spronken, The influence of gas density and liquid properties on bubble breakup, Chem. Eng. Sci. 48 (1993) 1213–1226.
[24] K. Akita, F. Yoshida, Bubble size, interfacial area, and liquid-phase mass transfer coefficient in bubble columns, Ind. Eng. Chem. Process Des. Dev. 13 (1974) 84–91.
[25] P. Wongsuchoto, T. Charinpenitkul, P. Pavasant, Bubble size distribution and gas–liquid mass transfer in airlift contactors, Chem. Eng. J. 92 (2003) 81–90.
[26] T. Miyahara, T. Hayashino, Size of bubbles generated from perforated plates in non-Newtonian liquids, J. Chem. Eng. Jpn. 28 (1995) 596–600.
[27] M. Fukuma, K. Muroyama, A. Yasunishi, Specific gas–liquid interfacial mass transfer coefficient in a slurry bubble column, J. Chem. Eng. Jpn. 20 (1987) 321–324.
[28] K. Ueyama, S. Morooka, K. Koide, H. Kaji, T. Miyauchi, Behaviour of gas bubbles in bubble columns, Ind. Eng. Chem. Process Des. Dev. 19 (1980) 592–599.
[29] W. Luewisutthichat, A. Tsutsumi, K. Yoshida, Bubble characteristics in multiphase flow systems: bubble sizes and size distributions, J. Chem. Eng. Jpn. 30 (1997) 461–466.
[30] T. Miyahara, A. Tanaka, Size of bubbles generated from porous plates, J. Chem. Eng. Jpn. 30 (1997) 353–355.
[31] J.P. Giovannettone, Hydrodynamics of a two-phase flow in a deep airlift reactor, Ph. D. Thesis, University of Minnesota, Minneapolis, Minnesota, 2005.
[32] N. Zuber, J.A. Findlay, Average volumetric concentration in two-phase flow systems, J. Heat Trans.-T. ASME Series C 87 (1965) 453–468.
[33] W.-D. Deckwer, I. Adler, A. Zaidi, A comprehensive study of CO_2-interphase mass transfer in vertical cocurrent and countercurrent gas–liquid flow, Can. J. Chem. Eng. 56 (1978) 43–55.
[34] M.H. Mobley, W.G. Brock, Widespread oxygen bubbles to improve reservoir releases, Lake Reservoir Manage. 11 (1995) 231–234.
[35] E. Camarasa, C. Vial, S. Poncin, G. Wild, N. Midoux, J. Bouillard, Influence of coalescence behaviour of the liquid and of gas sparging on hydrodynamics and bubble characteristics in a bubble column, Chem. Eng. Process. 38 (1999) 329–344.
[36] Z. Chen, C. Zheng, Y. Feng, H. Hofmann, Local bubble behavior in three-phase fluidized beds, Can. J. Chem. Eng. 76 (1998) 315–318.
[37] A.L. Urban, S.L. Hettiarachchi, K.F. Miller, G.P. Kincaid, J.S. Gulliver, Field experiments to determine gas transfer at gated sills, J. Hydraul. Eng.-ASCE 127 (2001) 848–859.
[38] H.M. Wadsworth, Handbook of Statistical Methods for Engineers and Scientists, McGraw-Hill, New York, NY, 1990.
[39] R.B. Abernathy, R.P. Benedict, R.B. Dowdell, ASME measurement uncertainty, J. Fluids Eng. 107 (1985) 161–164.
[40] W.L. Haberman, R.K. Morton, An experimental investigation of the drag and shape of air bubbles rising in various liquids Report, 802, Navy Department, The David W. Taylor Model Basin, 1953, NS715–102.
[41] T. Miyahara, Y. Matsuba, T. Takahashi, The size of bubbles generated from perforated plates, Int. Chem. Eng. 23 (1983) 517–523.
[42] L.W. Mays, Water Resources Engineering, John Wiley & Sons, Inc., New York, NY, 2001.